SLAC-PUB-9105
January 2002

# Qualitative analysis of the e-cloud formation *

S. Heifets
Stanford Linear Accelerator Center, Stanford University, Stanford, CA 94309

## Abstract

The qualitative analysis of the electron cloud formation is presented. Two mechanisms of the cloud formation, generation of jets of primary photo-electrons and thermalization of electrons in the electron cloud, are analyzed and compared with simulations for the NLC damping ring [1].

*Contributed to Ecloud'02 Mini-Workshop, 'Electron-Cloud Simulations for Proton and Positron Beams'*
*CERN, Geneva*
*April 15-18,2002*

*Work supported by Department of Energy contract DE–AC03–76SF00515.

# 1 Introduction

Since the discovery of instability at KEK photon factory [2], it was realized that the electron cloud can drive the fast multi-bunch [3] and single bunch instabilities [4] in the positron storage rings. The instabilities affect performance of the B-factories and design of the future linear colliders. Effects of the e-cloud on the beam dynamics is conveniently described by the effective wake field [5] which can be calculated [6] given the density of the e-cloud. The estimate of the density is the main difficulty of the problem. The e-cloud is neither static in time nor uniform in space and depends on the bunch population $N_b$, bunch spacing $s_b$, geometry of the beam pipe, the flux of the synchrotron radiation (SR) photons, and the yield of secondary electrons. Due to these difficulties, the density is usually determined either by elaborate simulations or considered as a fitting parameter. Nevertheless, it is highly desirable to have some analytic estimate of the density to interpret the results of simulations and for scaling of these results with machine parameters. The goal of the paper is to provide such an estimate. The results are compared with the simulations for the NLC [1].

We consider two mechanism of the e-cloud formation: the primary jets of the photo-electrons and thermalization of electrons in a part of the beam pipe. The paper is organized as following. In the next section, basic notions of the e-cloud are reminded. Then we consider jets of photo-electrons generated by the high flux SR. The density and the energy distribution are given for this mechanism. In Section 4, thermalization of electrons trapped in the self-consistent potential is considered. The e-cloud is described by Boltzmann distribution. The form of the self-consistent potential is found and the temperature of the distribution is determined from the condition of quasi-equilibrium. The applicability of such a model to the e-cloud interacting with a bunched beam is discussed. Effect of the multipactoring on the electron distribution is considered in Section 5 and the effect of the finite bunch length in Section 6. Finally, the threshold of the transverse coupled-bunch and the head-tail instability driven by the wake of the e-cloud is calculated in Section 7. Wherever it is possible, our results are compared with simulations [1].

As an example, we consider the e-cloud in the NLC main damping ring. The relevant parameters of the ring are listed in Table.

# 2 Steady-state: coasting beam, no SR

Let us start with the simplest case: a coasting beam with the average linear density $N_b/s_b$, a straight beam pipe with the beam pipe radius $b$, and no SR. Electrons of the cloud oscillate in the steady-state potential of the relativistic beam plus the space-charge potential of the cloud. Let us define the force $F$ and the potential $U$ by the equation of motion $d^2y/ds^2 = F = -\partial U/\partial y$,

| Parameter | Description | Value |
|---|---|---|
| $E$, (GeV) | beam energy | 1.98 |
| $N_b$ | bunch population | $1.5\,10^{10}$ |
| C, m | circumference | 299.92 |
| $s_b$, m | bunch spacing | 0.84 |
| $\sigma_z$, cm | bunch length | 0.36 |
| $\sigma_x$ $\mu$m | horizontal rms | 41.0 |
| $\sigma_y$ $\mu$m | vertical rms | 4.97 |
| $\delta$ | relative energy spread | $0.90910^{-3}$ |
| $b$, cm | beam pipe radius | 1.6 |
| $B$, T | dipole field | 1.2 |
| $L_b$, m | bend length | 0.96 |
| $L_d$, m | drift length | 0.975 |
| $E_0$, eV | peak of secondary electrons | 5.0 |
| $E_T$, eV | energy spread of secondary electrons | 2.0 |

Table 1: Parameters for the NLC main damping ring

where $s = ct$. Such a definition means that $U$ is measured in units of $mc^2$.

The force due to the beam at small distances $y << \sigma_y$ is linear in $y$,

$$F_b = -\frac{2r_e N_b y}{s_b \sigma_y(\sigma_x + \sigma_y)}. \tag{2.1}$$

It defines the average linear frequency $\bar{\Omega}_0/2\pi$ of the vertical electron oscillations

$$(\frac{\bar{\Omega}_0}{c})^2 = \frac{2r_e N_b}{s_b \sigma_y(\sigma_x + \sigma_y)}, \tag{2.2}$$

provided the space-charge force can be neglected. Here $r_e$ is the classical electron radius, $\sigma_{x,y}$ are the transverse rms size of the beam.

At large distances from the beam, $r >> \sigma_x$, the force rolls off as $1/r$ and the motion of electrons is non-linear. Approximate expression for the potential of the beam valid in the both extreme cases can be written as

$$U_{beam} = -\frac{N_b r_e}{s_b} \ln[\frac{b^2}{r^2 + \sigma_y(\sigma_x + \sigma_y)}]. \tag{2.3}$$

Interaction of electrons in the cloud with the density $n(r)$ adds the space charge potential (in units $mc^2$)

$$U_{SC} = 4\pi r_e[\int_0^b r'dr'n(r') \ln \frac{b}{r'} - \int_0^r r'dr'n(r') \ln \frac{r}{r'}]. \tag{2.4}$$

The Hamiltonian is $H(r, r', s) = (1/2)(v/c)^2 + U(r)$, $U = U_{beam} + U_{SC}$. Here we assumed the round pipe geometry.

Consider a simple example: the total potential calculated for the constant $n(r) = n_0$ is $U/(\pi n_0 r_e b^2) = 1 - (r/b)^2 - g \ln(b^2/r^2)$. The potential depends on $g = N_b/(\pi s_b b^2 n_0)$, the ratio of the densities of the beam and of the cloud

averaged over the beam pipe cross-section. The potential is shown in Fig.1. It has maximum at $r = r_m$, $r_m/b = \sqrt{g}$ and is monotonic for $g > 1$ within the beam pipe. For $g < 1$ it has maximum at the distance $r_m < b$, and the beam can not be stable: electrons go to the wall and the cloud decays. The condition $g = 1$ defines the maximum density

$$n_0 = \frac{N_b}{\pi s_b b^2}. \tag{2.5}$$

This is the well known condition of the neutrality. The condition formulated in this form is, actually, independent of the form of the distribution $n(r)$: the result Eq. (2.5) can be obtained directly from Eqs. (2.3),(2.4) if $n_0$ is understood as the average density of the cloud, $n_0 = (2/b^2) \int r dr n(r)$.

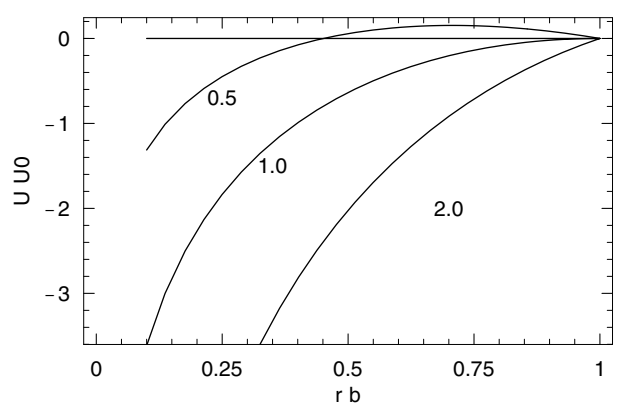


Figure 1: *Potential $U/U_0$ vs $r/b$, where $U_0 = \pi r_e n_0 b^2$. The values of the parameter $g = N_b/(\pi s_b b^2 n_0)$ are shown in the plot*

For the NLC parameters, $n_0 = 2.2\,10^7\ cm^3$. This agrees quite well with the results of simulations (M. Pivi) which give the average in time density at saturation $3.0\,10^7\ cm^{-3}$ at low level SR.

At the high level of the SR, the average density in simulations is higher, $6.\,10^7\ cm^{-3}$. This indicates that the average density not always is determined by the condition of neutrality and may depends on the level of the SR and the yield $\eta$ of the secondary electron emission. If the SR is strong (or, the photo-electric yield $\Upsilon$ is high), there is a high flux of primary photo-electrons with the density comparable or higher than that given by the condition of neutrality. Such a situation may be typical at high beam currents. In the extreme case, electrons go wall-to-wall between bunches. In this case, there is no electron cloud if it is understood as electrons oscillating many times before they hit the wall. The effect on the beam dynamics in this case may be different from the effect of the e-cloud. In the later case, the offset of the

leading bunch causes dipole oscillations of the cloud while in the first case the offset changes the velocity and the shortest distance to the beam of the ejected photo-electrons.

We consider two extreme cases: the low and the high level of the SR. The second case is simpler and it is considered in the next section.

# 3 The SR jets

The electrons in the beam pipe are mostly the primary photo-electrons and the secondary electrons. The multipactoring generates low-energy electrons with the energy distribution similar to that of the photo-electrons and they may be considered simultaneously.

In the case of a bunched beam, a kick to an electron at large distance $r >> \sigma_x$ is

$$\Delta(\frac{v}{c}) = -\frac{2N_b r_e}{r}. \tag{3.6}$$

A photo- electron produced at the wall sees the field of the parent bunch and starts moving toward the beam with the velocity $v/c = \sqrt{2E_0/mc^2} + 2N_b r_e/b$, where [1] $E_0 = 5$ eV. With the NLC parameters, the second term, approximately, doubles $v/c$. To the time of the arrival of the next bunch, the electron is at the distance 0.78 cm from the beam. It gets a kick from the second bunch, moves to location at the distance 0.94 cm on the other side from the beam and then hits the wall with the energy, approximately, 34 eV before the next bunch arrives. Such primary photo-electrons may explain the peak at $E \simeq 30$ eV obtained in simulations [1] with the high photo-electric yield $Y = 0.2$.

The secondary electrons don't see the parent bunch and have the starting velocity $v/c = \sqrt{2(E_0 \pm E_{spread})/mc^2}$ where [1] $E_{spread} \simeq 2$ eV. Such electrons are very close to the beam, at 2 mm when the second bunch arrives, and then hit the wall with the energy 446 eV, at the maximum of the yield of secondary electrons. The initial spread of energies is converted to the spread of energies of electrons hitting the wall in the range from 192 to 2135 eV.

These arguments are illustrated in Figs. 2 and 3 depicting results of the 1 dimensional tracking of 1000 particles generated initially at $r = b$ with random distribution in energy around 5 eV with rms spread 2 eV. A bunch is a sequence of 11 slices with population corresponding to Gaussian distribution within a bunch. Particles hitting a wall are replaced by a new particle distributed with energy spread 2 eV. Results in Fig. 3 show that high energy tails of the distribution are due to particles crossing the beam line and illustrate smearing of the initial jet into the e-cloud.

As we can see, the motion of electrons is very simple: electrons move in compact groups (jets), and there are, approximately, two jets within the beam pipe. The length of a jet is defined by the initial energy spread. The

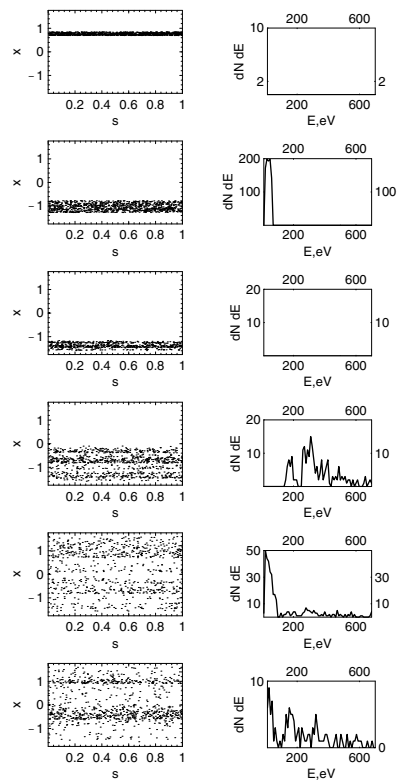


Figure 2: *Density profile $n(r)$ (left) and the energy distribution $dN/dE$ (right) of the lost electrons*

space-charge of the jets tends to produce an additional spread of the jet. However, if the beam current is high, the time of flight is short and the jet is smeared mostly due to the initial energy spread.

The density of the jets of primary photo-electrons is proportional to the number of photons

$$N_\gamma = \frac{5\alpha_0\gamma}{2\sqrt{3}}\frac{L_b}{R} \tag{3.7}$$

radiated by a positron in the bend with radius $R$ per pass, number of jets $k_{jets}$ within the beam pipe, and the volume of a jet. The density averaged over the length $L_d$ of the drift section where SR is absorbed and over the beam pipe cross-section, is

$$< n_{e\gamma} >= Y\frac{N_\gamma N_b}{\pi b^2 L_d}k_{jets}. \tag{3.8}$$

For the NLC parameters and $Y = 0.2$, $k_{jets} = 2$ and the average density $< n_{e\gamma} >= 5.5\,10^7\ 1/cm^3$. This is higher than the density $n_0$ given by the condition of neutrality and is very close to the result of simulations with the

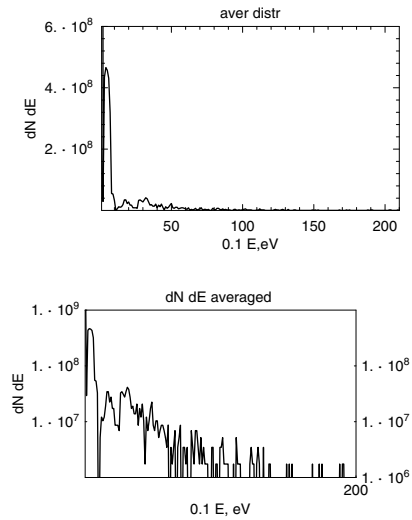


Figure 3: *Averaged over 10 passes energy distribution of the lost electrons (bottom: Log scale).*

large yield $Y$ of the primary photo-electrons.

In this case, the jets are the dominant contributor to the electron density. The space-charge field of the jets can clean the beam pipe kicking out electrons which may be produced by scattered photons or photo-ionization of the residual gas.

The density $n_{jet}$ in a jet crossing the beam line can be larger than the average density $< n_{e\gamma} >$. In simulation it was averaged over the area with the height $10\sigma_y$. With such a definition and $l_{jet} = 0.375$ mm defined by the energy spread, $n_{jet}$ is larger than $< n_{e\gamma} >$ by a factor $\pi b^2/(10\sigma_y l_{jet}) \simeq 4000$. In simulations this factor was about $10^3$ (M. Pivi).

The energy spread of the electrons is translated in some distribution over the shortest distances from the bunch and then in the distribution over the energy of electrons hitting the wall. Let us assume the uniform distribution of electrons along the jet. Then, if the shortest distance of the jet centroid from the beam line is $d$ and the length of the jet is $l_{jet}$, the energy $E(z)$ of an electron kicked to the wall depends on it location $z$ in the jet $|z| < l_{jet}/2$,

$$\frac{dN}{dE} = Y N_b N_\gamma \int \delta[E - \frac{mc^2}{2}(\frac{2N_b r_e}{d+z})^2]\frac{dz}{l_{jet}}. \tag{3.9}$$

Integration gives

$$\frac{dN}{dE} = \frac{Y N_b N_\gamma}{l_{jet}}\,(\frac{2N_b r_e}{mc^2})\,(\frac{mc^2}{2E})^{3/2}. \tag{3.10}$$

The distribution is shown in Fig. 4 for $Y = 0.2$.

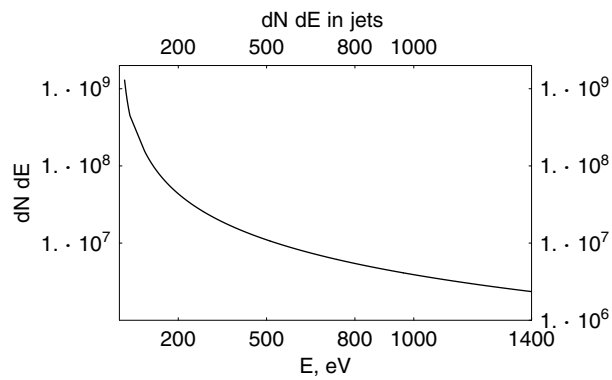


Figure 4: *Number of electrons $dN/dE$ hitting the wall per bunch. Electrons are accelerated by the beam while a jet crosses the beam line.* $Y = 0.2$

The high energy tail of the spectrum Eq. (3.10) of the electrons accelerated from the jets crossing the beam line depends on the beam current, beam pipe geometry, but also on the yield of the primary photo-electrons which may vary with the dose of radiation and many other factors. The low energy part of the spectrum in this mechanism is suppressed if the density of the electron cloud (electrons making many oscillations before hitting the wall) is low at large distances from the beam. It is true that the energetic electrons of the jets may produce large number of secondary electrons. The energy of such electrons, however, is low, of the order of $(mc^2/2)(2N_b r_e/b)^2 \simeq 7$ eV. Eventually, smearing of the jets leads to formation of the electron cloud.

# 4 Low SR flux, cloud formation

At the low beam current, electrons traveling from wall to wall experience many kicks from passing bunches. The kicks may change the electron direction making the motion, basically, random. Such electrons form the e-cloud. In practice, the number of random walks is not too large and the e-cloud is never stationary. Nevertheless, the e-cloud is a useful notion describing a possible extreme situation.

The phase space of electrons can be divided in three regions: one, in the vicinity of the beam, where a large kick from the beam sends electrons to the wall each time a bunch passes by. The size of this region is of the order of $r/b \simeq p_0$ where $p_0 = 2N_b r_e s_b/b^2$, an important parameter of the problem. It is clear that e-cloud may exists only if $p_0 << 1$. Otherwise, for $p_0 > 1$, most of electrons go wall-to-wall after each bunch passage. It is worth noting that, for the NLC, $p_0 = 0.277$ and would exceed one for $N_b$ by only a factor

of three larger than the NLC bunch population.

In the second region electrons move more or less randomly. The third region is in the vicinity of the wall. Generally, there is a bump of the potential well in the vicinity of the wall which defines how many of the secondary electrons can go to the central regions. Such a sheath works as a virtual cathode. The density in the sheath near the wall depends on the balance of the number of electrons kicked to the wall from the central region and the number of electrons produced at the wall by the SR and multipactoring.

## 4.1 Stationary e-cloud, averaged beam

In the zero approximation, the average beam potential at the distances $r >> \sigma_\perp$ depends only on the bunch spacing,

$$U_b(r) = -\frac{2N_b r_e}{s_b} \ln(\frac{b}{r}). \tag{4.11}$$

The average over time distribution function of electrons trapped in this potential well can be taken as Boltzmann distribution

$$\rho(r, v) = |N| e^{-\frac{1}{T}[(1/2)(v/c)^2 + U(r)]}, \tag{4.12}$$

where $T$ is temperature in units of $mc^2$, $|N|$ is the normalization factor, $\int 2\pi r dr dv \rho(r, v) = \pi b^2 n_0$. The density of the cloud

$$n_{cl}(r) = \int dv \rho = |N| c\sqrt{2\pi T} e^{-U/T} = n_0 \frac{b^2}{2} \frac{e^{-U/T}}{\int r dr e^{-U(r)/T}}. \tag{4.13}$$

Here $n_0 = (b^2/2) \int r dr n_{cl}$ is the average density of the cloud to be defined.

The potential $U$ in Eq. (4.13) is the total potential $U = U_b + U_{cl}$ of the beam and the cloud. The later is defined by the Poisson equation with the right-hand-side (RHS) proportional to $n_{cl}$. Let us define dimensionless $x = r/b$ and measure all potentials in units of $T$, introducing $V(x) = (U(r)/T)_{r=bx}$. Then, for a cylindrically symmetric beam pipe, the Poisson equation takes the form

$$\frac{1}{x} \frac{\partial}{\partial x} x \frac{\partial V_{cl}}{\partial x} = -\hat{g} \frac{e^{-V(x)}}{\int x dx e^{-V(x)}}, \tag{4.14}$$

where

$$V(x) = V_{cl} - g \ln(1/x), \quad g = \frac{2N_b r_e}{T s_b}, \quad \hat{g} = \frac{2\pi r_e b^2}{T} n_0. \tag{4.15}$$

In the stationary case, the total potential $U(r)$ and the force $dU(r)/dr$ are zero at $r = b$. That gives the boundary conditions $V(1) = 0$, $(dV/dx)_{x=1} = 0$ or, for the space-charge potential,

$$V_{cl}(1) = 0, \quad (\frac{dV_{cl}}{dx})_{x=1} = -g. \tag{4.16}$$

The space-charge potential is finite at $x = 0$. Integration of Eq. (4.14) with the weight $x$ gives $(dV_{cl}/dx)_{x=1} = -\hat{g}$. Comparison of this result with Eq. (4.16) gives $\hat{g} = g$ and defines the average density

$$n_0 = \frac{N_b}{\pi s_b b^2}, \tag{4.17}$$

reproducing the density given by the condition of neutrality. Note, that the average density $n_0$ is independent of the shape of the density $n_{cl}(r)$ and temperature $T$.

Potentials $V(x)$, $V_{cl}(x)$, and

$$n_{cl} = \frac{n_0}{2} \frac{e^{-V(x)}}{\int_0^1 x dx e^{-V(x)}} \tag{4.18}$$

depend only on one parameter $g$. It is defined in the next section.

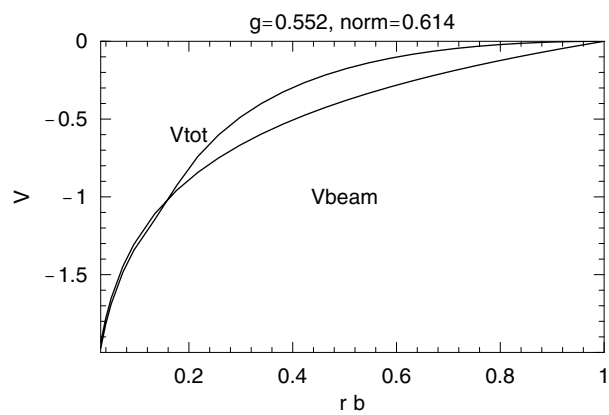


Figure 5: *Total self-consistent potential $V(x)$ and the beam potential $V_b = -g\ln(1/x)$ vs $x = r/b$. Parameter $g$ is found from Eq. (4.23).*

## 4.2 Stationary distribution, bunched beam

In the approximation of the averaged beam potential, electrons have regular motion oscillating in the self-consistent potential well. However, for the NLC DR, $\bar{\Omega}_{0,y}/2\pi = 31.7$ GHz and the number of oscillations between bunches $\bar{\Omega}_{0,y} s_b/(2\pi c) >> 1$. The linear frequency of oscillations during the bunch passage $\Omega_B$ is higher $\sqrt{s_b/\sigma_z}$ times. Even the number of oscillations per

bunch length $\Omega_B \sigma_z/c$ is large, $n_{osc} = 3.67$. Obviously, the beam potential cannot be approximated by a potential of the coasting beam.

Nevertheless, an electron shifts its position between bunches only by the distance $2N_b r_e s_b/b = p_0 b \simeq 0.27\, b$. Hence, before an electron can reach the wall, it is kicked several times. Electrons move changing direction and the motion is similar to a random walk. We can estimate the number of kicks $n_{pass}$ an electron gets before it can reach the wall from

$$n_{pass} < (\frac{2N_b r_e s_b}{r})^2 >= b^2, \tag{4.19}$$

what gives $n_{pass} \simeq 1/p_0$. It is clear again that it makes sense to speak about e-cloud only for $p_0 << 1$. For the NLC parameters, $p_0 \simeq 3 - 4$.

In the previous section, the temperature $T$ remains undefined. Now we take into account the beam bunching considering bunches as point-like macro particles. The goal is to define the temperature $T$ and the average over time density of the cloud.

The bunching of the beam has several implications. First, instead of the steady-state beam potential, an electron in the beam pipe sees periodic kicks. Neglecting the space-charge potential, we can write a simplectic map $M(x, v)$ giving transformation of the electron coordinates per bunch spacing $[x, v] - > [\bar{x}, \bar{v}] = M(x, v)[x, v]$. The eigen values of the Jacobian $D[M[x, v], \{x, v\}]$ are real only for $x < \sigma_\perp/b$, i.e. in the region of the linear motion.

Elsewhere the motion is chaotic and the average in time distribution function can be taken in the form of Eq. (4.12) although the approximation of the coasting beam is not valid. That is possible due to the other effects of the bunched beam: heating of the cloud caused by the kicks balanced by the cooling of the cloud due to the loss of electrons.

A kick from a bunch increases the average energy of the e-cloud by

$$\Delta E_{gain} = 2\pi \int r dr dv \rho(r, v)(\frac{2N_b r_e}{r})^2, \tag{4.20}$$

where integration is over the phase space of the cloud.

The electrons in the vicinity of the beam are kicked to the wall and are replaced with the low energy secondary electrons. The later process produces cooling. To be lost, an electron has to reach the wall before the next bunch arrives. The trajectory of an electron between bunches can be estimated as following. Consider an electron with the initial conditions $r, v/c$ just before a bunch arrives. A bunch changes $\beta = v/c$ to $\beta_0 = v/c - 2N_b r_e/r$. After that, an electron moves in the field of the space charge. Let us assume, for a moment, a uniform density of the cloud, $n_{cl}(r) = n_0$. Then, the space-charge force is $2\pi r_e n_0 r$ and the electron is at $\bar{r} = r\cosh(\Omega s_b/c) + (c\beta_0/\Omega)\sinh(\Omega s_b/c)$ at the time of arrival of the next bunch. Here $(\Omega/c)^2 = 2\pi n_0 r_e$. A quasi-stationary cloud can exist only if $(\Omega s_b/c)^2 = p_0 << 1$. For the NLC parameters, $n_0 = 2.2\, 10^7\ cm^{-3}$, and $(\Omega s_b/c)^2 = 0.277$. In the case of small $(\Omega/c)$,

$\bar{r} = r + (v/c - 2N_b r_e/r)s_b$ and is independent on $n_0$. The electron hits the wall if $|\bar{r}| > b$, or

$$\frac{v}{c} > \frac{b-r}{s_b} + \frac{2N_b r_e}{r}, \quad \text{or} \quad \frac{v}{c} < -\frac{b+r}{s_b} + \frac{2N_b r_e}{r}. \tag{4.21}$$

All electrons within this part of the phase space get lost and are replaced by the electrons from the cloud. The energy loss is equal to the energy of the lost particles before they were kicked to the wall:

$$\Delta E_{loss} = 2\pi \int r dr dv \rho(r,v)[\frac{1}{2}\frac{v^2}{c^2} + U(r)], \tag{4.22}$$

where integration is restricted by the condition Eq. (4.21) and $0 < r < b$. Here we neglected the energy brought to the cloud by the low energy secondary electrons coming in from the wall.

The balance of energies Eq. (4.20) and Eq. (4.22) gives the following equation:

$$gp_0 \int_0^1 \frac{dx}{x} e^{-V(x)} F(x) = \int_0^1 x dx e^{-V(x)}[(\frac{1}{2}+V(x))(1-F(x))+\frac{1}{2\sqrt{\pi}}(z_+ e^{-z_+^2}+z_- e^{-z_-^2})], \tag{4.23}$$

where

$$F(x) = (1/2)(Erf[z_+] + Erf[z_-]), \quad p_0 = 2N_b r_e s_b/b^2, \tag{4.24}$$

and

$$z_+ = \sqrt{\frac{g}{2p_0}}(1 - x + \frac{p_0}{x}), \quad z_- = \sqrt{\frac{g}{2p_0}}(1 + x - \frac{p_0}{x}). \tag{4.25}$$

Let us remind that, given $p_0$, $V(x)$ depends only on $g$. Eq. (4.23) defines $g$, i.e. the temperature $T$. It is plausible to expect that $g \simeq 1/\ln(1/p_0)$. Given $p_0$, the solution of Eq. (4.14) and Eq. (4.23) can be obtained numerically. Calculations for the NLC parameter $p_0 = 0.277$ define $g = 0.552$, what is close to the estimate above, $1/\ln(1/p_0) = 0.780$. The temperature in units of $mc^2$ is $T = g(2N_b r_e/s_b)$, or $T = 92.4$ eV. The potential $V(x)$ is shown in Fig. 5. At small distances it goes as beam potential but at large distances is flatter due to the space charge contribution. The density profile $n(x)/n_0$, Eq. (4.18), for the same parameters is shown in Fig. 6. The density at the beam line (at the moment of a bunch arrival) is substantially larger that the average density $n_0$.

The number of electrons with the energy $E$ hitting the wall of the drift chamber with the length $L_d$ is

$$\frac{dN(E)}{dE} = 2\pi L_d \int r dr dv \rho(r,v)\delta[\frac{1}{2}(\frac{v}{c} - \frac{2N_b r_e}{r})^2 + U(r) - E], \tag{4.26}$$

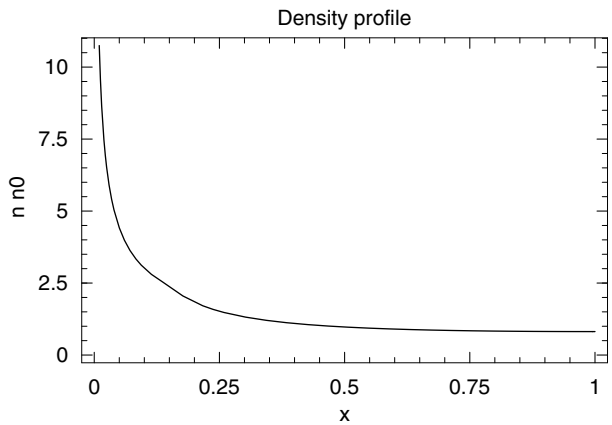


Figure 6: *The density* $n(r)/n_0$, $n_0 = 2.2\,10^7\ cm^{-3}$ *vs* $x = r/b$ *for the NLC parameter* $2N_b r_e s_b/b^2 = 0.277$.

where integration is taken over the region $v/c > \sqrt{2T}z_+$ and $v/c < -\sqrt{2T}z_-$, and $\rho$ is the distribution function at the moment of bunch arrival.

Substitution of $\rho(r,v)$ and $V(x)$ gives

$$\frac{dN(E)}{dE} = \frac{n_0}{T}\frac{\sqrt{\pi}}{2}\frac{L_d b^2}{\int_0^1 xdxe^{-V(x)}}\int_0^1 \frac{xdx}{\sqrt{E/T - V(x)}}G(x)e^{-V(x)}, \qquad (4.27)$$

where

$$\begin{aligned} G(x) = \quad & e^{-(\frac{1}{x}\sqrt{\frac{p_0 g}{2}}+\sqrt{\frac{E}{T}-V})^2}\Theta[\sqrt{\frac{E}{T}-V(x)} - (1-x)\sqrt{\frac{g}{2p_0}}] \\ & +e^{-(\frac{1}{x}\sqrt{\frac{p_0 g}{2}}-\sqrt{\frac{E}{T}-V})^2}\Theta[\sqrt{\frac{E}{T}-V(x)} - (1+x)\sqrt{\frac{g}{2p_0}}], \qquad (4.28) \end{aligned}$$

and $\Theta[z]$ is a step function.

The result of calculations is shown in Fig. 7. Parameters are the same as in Fig. 6.

Finally, the number of electrons hitting the wall per passing bunch is given by the integral

$$N_{loss} = 2\pi L_d \int rdrdv\rho(r,v) \qquad (4.29)$$

where the integration is over the region $v/c > \sqrt{2T}z_+$ and $v/c < -\sqrt{2T}z_-$. In terms of the total potential $V(x)$, $dN_{loss}/ds$ is given as

$$N_{loss} = \frac{N_b}{s_b}\frac{L_d}{\int_0^1 xdxe^{-V}}\int_0^1 xdxe^{-V(x)}[1 - F(x)]. \qquad (4.30)$$

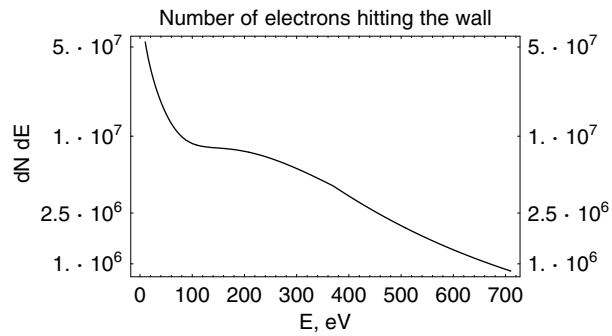


Figure 7: *Number of electrons per bunch $dN/dE$ $1/eV$ accelerated from the e-cloud and hitting the wall with energy $E$.*

$F(x)$ is defined by Eq. (4.24). Calculation gives $N_{loss} = 5.53\,10^9$, 31% of the total $N_{tot} = \pi b^2 L_d n_0 = 1.74\,10^{10}$ electrons in the cloud in the drift with length $L_d$. This result may be compared with the simple estimate which assumes that all particles within radius $r$, where $(2N_b r_e/r)s_b > b$ are lost. If the density would be constant $n_0 = 2.2\,10^7\ 1/cm^3$, then $N_{loss} = 1.37\,10^9$. The actual number is higher because the density at the beam line is higher than the average density $n_0$.

The total energy loss is given by the integral

$$\frac{E_{loss}}{T} = \frac{\pi b^2 n_0}{\int_0^1 xdxExp[-V(x)]} \int xdxe^{-V(x)} \int due^{-u^2}[(u - \frac{1}{x}\sqrt{\frac{p_0 g}{2}})^2 + V(x)]. \tag{4.31}$$

Here the variable $u = (v/c)/\sqrt{2T}$, and the integral is taken over $|x + u\sqrt{2p_0/g} - p_0/x| > 1$. Numeric integration gives power loss $(c/s_b)E_{loss} = 101$ $W/m$.

# 5 Saturation

High energy electrons hitting the wall produce secondary electrons which, after thermalization, may increase the density of the cloud in the avalanche-like way. Let us estimate the number of bunches $m$ needed to reach saturation of the cloud density $n_0 = 2.2\,10^7\ 1/cm^3$. At the low level of the photo-electric yield $Y = 0.002$ taken in simulations [1], the SR adds to the average density $n_{SR} = 5.5\,10^5\ 1/cm^3$ per bunch (see Eq. (3.8). Most of these electrons go wall-to-wall and only $(\eta - 1)n_{SR}$ of the secondary electrons remain in the

cloud. Due to the multipactoring the density increases exponentially:

$$\frac{dn}{dm} = -\xi n + \eta\xi n + (\eta - 1)n_{SR}, \quad n = \frac{n_{SR}}{\xi}[e^{\xi(\eta-1)m} - 1]. \tag{5.32}$$

Here we introduced parameter $\xi = N_{loss}/N_{tot}$ defining the fraction of the cloud participating in multipactoring. The estimate of the previous section gives $\xi = 0.3$ and the density reaches saturation after

$$m = \frac{1}{\xi(\eta - 1)} \ln[\frac{n_0}{n_{SR}}\xi + 1] \tag{5.33}$$

passes. For the NLC DR, $m = 19$ for $\eta = 1.45$. At the high SR photon flux, where $n_{SR} \simeq n_0$, the number of passes to reach saturation os of the order of $[\xi(\eta - 1)]^{-1} \simeq 7$. These estimates are in reasonable agreement with the simulations.

# 6 Effect of the multipactoring

In the equilibrium, the number of lost particles is equal to the particles coming to the cloud from the wall. If the yield of secondary electrons is high, to sustain the equilibrium, the total potential changes to stop the back flow of the secondary electrons.

The distribution function $\rho(r, v)$ satisfies the Liouville equation with the source $S$,

$$\frac{\partial\rho}{\partial t} + v\frac{\partial\rho}{\partial r} - c^2\frac{\partial U(r)}{\partial r}\frac{\partial\rho}{\partial v} = S\frac{\delta(r - b)}{2\pi r}f(v). \tag{6.34}$$

Here $f(v)$ is normalized distribution of the secondary electrons over velocity,

$$f(v) = \frac{v}{c^2 T_w}e^{-\frac{v^2}{2c^2 T_w}}, \quad \int_{-\infty}^{0} dv f(v) = 1. \tag{6.35}$$

The temperature $T_w$ is equal to the average energy of secondary electrons $E_0$ in units of $mc^2$, $T_w = \int dv(v^2/2c^2)f(v)$. In the estimate we assume $E_0 = 2$ eV, $T_w = 4.0\,10^{-6}$. The source $S_{cl}$, the number of secondary electrons ejected from the wall per unit time and unit length of the beam pipe, is given by the number of lost electrons $dN_{loss}/ds$ and the yield of the secondary electrons $\eta$, $S_{cl} = (\eta - 1)(c/s_b)dN_{loss}/ds$. (More exactly, $S_{cl}$ is given only by the lost particles with the sufficiently high energy, $E > 50$ eV). If there is the SR flux, it adds $S_{SR}$, $S = S_{cl} + S_{SR}$,

$$S_{SR} = Y N_\gamma N_b \frac{c}{s_b L_d}. \tag{6.36}$$

We imply here that electrons generated at the wall are thermalized and are added to the e-cloud. This process works as a sink for the generated electrons and allows us to consider the average in time electron density $\rho(r,v) = \rho_{cl}(H) + \rho_s(r,v)$, where $H = v^2/2c^2 + U(r)$. Here the first term is the distribution function of the cloud and the second term describes secondary electrons,

$$\rho_s(r,v) = \frac{S}{2\pi b}\frac{f(c\sqrt{2H})}{c\sqrt{2H}}\Theta(b-r). \tag{6.37}$$

The density of the secondary electrons $n_s = \int dv \rho_s$ at the wall is

$$n_s(r) = \frac{S}{2bc\sqrt{2\pi T_w}}. \tag{6.38}$$

The total potential at the wall $V(1) = 0$, and in the vicinity of the wall can be expanded in series $V(x) = (1-x)V_1 + (1-x)^2(V_2/2) + ...$ To have maximum at $x_{max} < 1$, $V_2$ has to be negative. The potential is maximum $V_{max} = -V_1^2/(2V_2)$ at the distance $\Delta = (1 - x_{max}) = -V_1/V_2$ from the wall. Hence, $V_1 > 0$. The Poisson equation at $x \to 1$ relates the coefficients $V_1$, and $V_2$, $V_2 - V_1 = -G$, where

$$G = S\frac{r_e b}{cT}\sqrt{\frac{2\pi}{T_w}} + \frac{2\pi r_e b^2 n_0}{T\int_0^1 x dx exp[-V(x)]}. \tag{6.39}$$

The second term in the right-hand-side is due to the density of the cloud.

To stop secondary electrons to go into the beam pipe, the maximum of the potential $V_{max}$ has to be of the order of $T_w/T$. $V_{max}$ can be estimated equating the number of particles returning to the cloud to $dN_{loss}/ds$. Electrons that go back into the beam pipe have to have energy $v^2/(2c^2) > TV_{max}$,

$$(\frac{dN}{ds})_{back} = \frac{s_b}{c}\int_{v/c<-\sqrt{2TV_{max}}} 2\pi r dr dv S f(v)\frac{\delta(r-b)}{2\pi r} = \frac{s_b}{c} S e^{-V_{max}T/T_w}. \tag{6.40}$$

Substituting $S$ and equating that to $(dN/ds)_{loss} = N_{loss}/L_d$ defined by Eq. (4.30), we get

$$V_{max} = \frac{T_w}{T}\ \ln[\eta + \frac{YN_\gamma N_b}{N_{loss}}]. \tag{6.41}$$

This defines $V_1 = V_2 + G$ and $\Delta = -V_1/V_2$,

$$\Delta = \frac{-V_{max} + \sqrt{V_{max}^2 + 2GV_{max}}}{V_{max} + G - \sqrt{V_{max}^2 + 2GV_{max}}}. \tag{6.42}$$

This result has meaning only if $\Delta << 1$, i.e. for the large enough density of the cloud. Otherwise, the height of the potential barrier can not reach $T_w$ and the density keeps building up.

If $G << V_{max}$,

$$\Delta = \frac{2V_{max}}{G}. \tag{6.43}$$

For the NLC parameters and $\eta = 1.45$, $\Delta = 0.082$ and $V_{max} = 0.032$ or 2.95 eV.

Although the height of the potential bump at the $r_{max} = b(1-\Delta)$ is small, of the order of $T_w$, it changes the equilibrium density of the cloud. To see the effect on the average density, let us again integrate the Poisson equation

$$\frac{1}{r}\frac{d}{dr}r\frac{dU_{cl}}{dr} = -4\pi r_e n_{cl}(r) \tag{6.44}$$

over r with the weight r in the interval $0 < r < r_{max}$. Because $U_{cl}$ is finite at $r = 0$, we get for the average density

$$< n_{cl} >\equiv \frac{2}{r_{max}^2}\int_0^{r_{max}} n_{cl}(r)rdr = -\frac{1}{2\pi r_{max}}(\frac{dU_{cl}}{dr})_{r=r_{max}}. \tag{6.45}$$

The total potential $U(r) = U_{cl} - gT\ln(b/r)$ is maximum at $r = r_{max}$. Therefore, $(\frac{dU_{cl}}{dr})_{r=r_{max}} = -gT/r_{max}$, and

$$< n_{cl} >= \frac{gT}{2\pi}(\frac{1}{r_{max}})^2. \tag{6.46}$$

Substitution of $g$ from Eq. (4.15) and $r_{max} = b(1-\Delta)$ gives

$$< n_{cl} >= n_0(\frac{1}{(1-\Delta)})^2. \tag{6.47}$$

The average density is higher than that given by the condition of neutrality but the difference is small provided $\Delta << 1$.

It is worth noting that, without the potential barrier, primary photoelectrons with positive energy go above the potential well. They add to the average density of electrons but their space charge reduces the density of the cloud in such a way that the total average density is still given by the condition of neutrality.

Electrons reflected by the potential barrier hit the wall again increasing the power deposited to the wall. The power deposited by this mechanism depends on the yields,

$$\frac{dP}{ds} = \frac{c}{s_b}T_w[(\eta-1)\pi b^2 n_0\frac{N_{loss}}{N_{tot}}+YN_\gamma\frac{N_b}{L_d}][1-(1+V_{max}\frac{T}{T_w})e^{-V_{max}T/T_w}]. \tag{6.48}$$

For the NLC DR this contribution is negligible, less than W/m.

Another effect of the secondary electrons trapped at the wall is the introduction of a small azimuthal asymmetry of the potential well for the beam particles. The dipole component of such perturbation may cause an orbit distortion and the quadrupole component leads to the asymmetric dependence of the tune on the beam current. The estimate shows, however, that these effects are small.

# 7 Effect of the finite bunch length

We assumed everywhere above that a bunch can be described as a point-like macro particle. The finite bunch length may substantially change the number of lost particles from the region near the beam. As it was mentioned in Section 2, the number of oscillations within the bunch length for such electrons is large. (It may be not true for the electrons far away from the beam because the frequency of oscillations decreases with amplitude). The field of a bunch at a given location around the ring varies slowly compared to the period of oscillations and can be considered as an adiabatic perturbation. As it is well known, the amplitude of oscillations in this case returns to the initial value when the perturbation is turned off. It means, that an electron may decrease the amplitude of oscillations while bunch is passing by, but retains the initial velocity and position after the bunch goes away. These arguments mean that the number of the high energy electrons hitting the wall and power deposition are smaller for the larger bunch length. On the other hand, low energy electrons in vicinity of the beam can live there for a long time what would mean larger density at the beam line. From this point of view, it is preferable to have short bunches but with a large bunch current to be in the regime where electrons go wall-to-wall in one pass.

One of implications of the finite bunch length is the betatron tune variation along the bunch. The kick from the head of a bunch causes motion of the e-cloud electrons toward the beam line and increases density of e-cloud in the tail of the bunch. The tune spread is of the order of the tune shift:

$$\Delta Q = \frac{2\pi r_e n_0 < R >^2}{\gamma Q}, \tag{7.49}$$

where $< R >$ is the average machine radius. The tune spread for the NLC is large, $\Delta Q = 0.0207$ at $n_0 = 2.22\,10^7\ 1/cm^{-3}$. The interaction with the dense jets can change tune of the bunches in the head of the bunch train differently than for the rest of the bunches causing tune variation along the bunch train.

# 8 Effect on the wake field

Let us consider the cloud with the average density $n_0$ defined by the condition of neutrality. The wake field of the cloud can be estimated analytically [5, 6]. For a long bunch, the short-range wake per unit length has the form of a single mode

$$W_{bunch}(z) = W_m \frac{n(p_0)s_b}{N_b}(\frac{\Omega_B}{c})\sin(\mu\zeta)e^{-\frac{\mu\zeta}{2Q}}, \tag{8.50}$$

where the e-cloud density is taken at $r_{min} = bp_0$ defined as $(2N_b r_e/r_{min})s_b = b$ to take into account that the density at the beam line is larger than average density, $\Omega_B/2\pi$ is the linear bunch frequency of oscillations,

$$(\frac{\Omega_B}{c})^2 = \frac{2N_b r_e}{\sigma_y(\sigma_x + \sigma_y)\sigma_z\sqrt{2\pi}}, \tag{8.51}$$

$\zeta = \Omega_B z/c$, and $W_m$, $\mu$ and $Q$ are characteristics of the wake with weak dependence on the aspect ratio $\sigma_y/\sigma_x$ and the beam pipe aperture. They were calculated in the reference [6]: $W_m = 1.2$, $\mu = 0.9$, and $Q = 5$.

The bunch shunt impedance per turn

$$\frac{R_s^{bunch}}{Q} = 2\pi R \frac{Z_0}{4\pi} \frac{n(p_0)s_b}{N_b} W_m \tag{8.52}$$

is $\simeq 94$ MOhm/m.

## 8.1 Transverse coupled bunch instability

For a single bunch stability, $\Omega_B/c = 45.3\ 1/cm$ and $W_{max} = 1.55\,10^4\ cm^{-2}$.

To consider the CB instability, the long-range (LR) wake has to be scaled from the short-rane wake Eq. (8.50) replacing the bunch length by $s_b$ and, secondly, using the average density $n_0$. The maximum value of the LR wake is:

$$W_{LR}(z) = W_m \frac{n_0 s_b}{N_b} (\frac{\Omega_{beam}}{c}) e^{-\frac{\mu\zeta}{2Q}}, \tag{8.53}$$

where

$$(\frac{\Omega_{beam}}{c})^2 = \frac{2N_b r_e}{s_b r_{min}^2}. \tag{8.54}$$

The period of the LR mode $2\pi/(\Omega_B/c)_{LR} = 4.7$ bunches.

The LR shunt impedance per turn

$$\frac{R_s^{beam}}{Q} = 2\pi R \frac{Z_0}{4\pi} \frac{n_0 s_b}{N_b} W_m \tag{8.55}$$

is $\simeq 67$ MOhm/m for the NLC DR nominal parameters in good agreement with simulations [1].

The maximum growth rate of the transverse CB

$$\frac{1}{\tau} = \frac{I_{beam} R_s^{beam}}{(E/e)} \frac{c_0 \beta_y}{4\pi R} e^{-(\Omega/c)_{beam}\sigma_z)^2} \tag{8.56}$$

is $\tau = 0.01$ ms.

## 8.2 Head-Tail instability

The growth rate of the head-tail instability can be determined using Satoh-Chin formalism [7]. The result of calculations are shown in Figs. 8,9. Fig. 8 depicts results of calculations for the wake oscillating with the frequency $\Omega_B$ defined by the bunch density. The cloud density is given by the condition of neutrality. The instability exists only in a narrow range of the bunch current.

Dependence on the bunch current is unusual: the instability has a low threshold but beam is stabilized at higher currents. This may be related to the fact that the amplitude and the resonance frequency of the wake depend on the beam current contrary to the usual geometric wake fields.

In particular, the resonance frequency grow with the current and can go out of the bunch spectrum. This result should be checked with tracking simulations.

Fig. 9 show results for the wake oscillating with the frequency reduced by a factor of 10 (what is close to $\bar{\Omega}_0$). In this case, instability exists in much wider range of the bunch current.

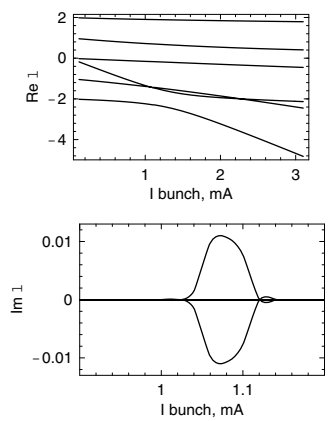


Figure 8: *Head-tail instability of a single bunch driven by the electron cloud. The growth rate* $Im[\lambda] = 1/(\omega_s \tau)$ *and the coherent tune shift* $Re[\lambda] = \omega/\omega_s$. *The wake frequency is given by the average bunch density.*

# 9 Summary

A simple model of the e-cloud formations allows us to reproduce main results obtained in simulations. Two mechanisms of the e-cloud formation are considered explaining the level of the density at saturation. The jets of primary and secondary electrons can explain the high energy tail in the distribution of electrons hitting the wall. The density of the jets at high beam current can

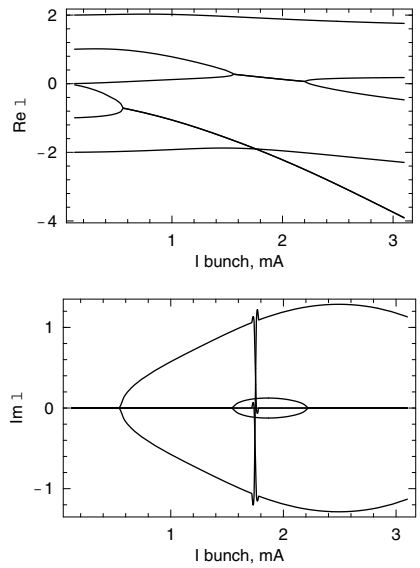


Figure 9: *The same as in previous figure but the wake oscillates with frequency defined by the average beam density (i.e. factor 10 lower).*

be, actually, higher then that given by the condition of neutrality. At high currents, electrons may go wall-to-wall between bunches and electron cloud, in the usual sense, does not exist. The beam stability depends in this case on the perturbation due to few jets within the beam pipe. Thermalization of electrons, takes place at a moderate current within some distances from the beam. Even if the number of the linear oscillations per bunch is large, such electrons can be described by the Boltzmann distribution due to randomness of the electron motion. The temperature of the distribution is defined by the condition of the energy equilibrium. The multipactoring does not change the temperature much but rather affects the distribution of electrons in the vicinity of the wall. That explains why the average density of the cloud is close to that given by the condition of neutrality. The final bunch length may change the power deposited to the wall and the density of electrons at the beam line. Interaction with the cloud can cause the tune variation along the bunch train. Transverse CB instability requires strong feedback. The head-tail instability which can not be cured by the feedback contrary to the coupled bunch instability. However, the instability is suppressed due to high frequency of the wake.

## Acknowledgments

I thank M. Pivi for providing us with the results of his simulations and T. Raubenheimer for initiating this study.

# References


[1] Mauro Pivi and M. Furman, Electron cloud in the NLC damping ring, LBNL, Sptember 17, 2001 (unpublished)

[2] Izawa, Y. Sato, and T. Toyomasu, "The Vertical Instability in a Positron Bunched Beam," Phys. Rev. Lett. **74** 5044 (1995).

[3] K. Ohmi, "Beam-Photoelectron Interactions in Positron Storage Rings," Phys. Rev. Lett. **75** 1526 (1995).

[4] H. Fukuma *et al.*, "Observation of Vertical Beam Blow-up in KEKB Low Energy Ring." Proc. EPAC, Vienna, Austria , 2000, p. 1124.

[5] K. Ohmi and F. Zimmermann, "Head-Tail Instability Caused by Electron Clouds in Positron Rings," Phys. Rev. Lett. **85** 3821 (2000).

[6] S. Heifets, Wake field of the e-cloud, SLAC-PUB-9025, 11/2001

[7] K. Satoh and Y.H. Chin, "Transverse Mode Coupling in a Bunched Beam," Nucl. Instr. Meth. **207**, 309 (1983).


# 10 Appendix: examples

| Parameter | Description | Value |
|---|---|---|
| $E$, (GeV) | beam energy | 1.98 |
| C, m | circumference | 299.792 |
| $\beta_x$, m | horizontal | 3.64 |
| $\beta_y$, m | vertical | 7.06 |
| $\nu_x$, m | horizontal tune | 27.261 |
| $\nu_y$, m | vertical tune | 11.136 |
| $\nu_s$ | synch.tune | 0.0035 |
| $b$, cm | beam pipe radius | 1.6 |
| $B$, T | dipole field | 1.2 |
| $L_b$, m | bend length | 0.96 |
| $L_d$, m | drift length | 0.975 |
| $E_0$, eV | peak of secondary electrons | 5.0 |
| $E_T$, eV | energy spread of secondary electrons | 2.0 |
| $Y$, | photo-electric yield (low/high SR) | 0.002/0.2 |
| $\eta$, | secondary emission yield, | 1.45 |

Table 1: Global parameters for the NLC main damping ring

| Parameter | Description | I | II | III | IV |
|---|---|---|---|---|---|
| $s_b$, m | bunch spacing | 0.84 | 0.42 | 0.84 | 0.42 |
| $N_b$ $10^{10}$ | bunch population, | 1.5 | 0.75 | 1.5 | 0.75 |
| $e_{x,N}$, mm mrad | norm. x-emitt. | 3.86 | 3.86 | 150.0 | 150.0 |
| $e_{Y,N}$, mm mrad | norm y-emitt. | 0.018 | 0.018 | 150.0 | 150.0 |
| $\sigma_z$, mm | rms bunch length | 3.6 | 3.6 | 7.0 | 7.0 |
| $\delta\, 10^{-3}$ | relat. energy spread | 0.909 | 0.909 | 10.0 | 10.0 |

Table 2: Four sets of parameters for the NLC main damping ring

| Parameter | Description | Simul. | I | II | III | IV |
|---|---|---|---|---|---|---|
| $I_{beam}$, Amp | aver.beam current | 0.86 | 0.86 | 0.86 | 0.86 | 0.86 |
| $n_0$, $10^{13}\, m^{-3}$ | average density | 3.0 | 2.2 | 2.2 | 2.22 | 2.22 |
| $n_{eff}$, $10^{13}\, m^{-3}$, | effective density | | 3.11 | 11.9 | 3.11 | 11.9 |
| Number of y-oscill/bunch | | | 7.16 | 5.06 | 0.283 | 0.20 |
| $f_{beam}$, MHz | LR wake frequency | | 76.28 | 305.14 | 76.28 | 305.24 |
| $f_{beam}/f_{rev}$ | | 100-200 | 76.23 | 304.9 | 76.23 | 304.9 |
| $W_{LR}$ period in $s_b$ | | 4 | 4.7 | 2.34 | 4.7 | 2.34 |
| $W^y_{bunch}$ $m^{-2}$ | short range $W_{max}$ | | $3.12E9$ | $8.5E9$ | $6.3E7$ | $1.7E8$ |
| $W^y_{beam}$ $10^6\, m^{-2}$ | LR $W_{max}$ | 0.60 | 0.715 | 2.86 | 0.715 | 2.86 |
| $R^y_s$ MOhm/m | SR shunt | | 94.07 | 361.5 | 94.06 | 361.6 |
| $R^y_s$ MOhm/m | LR shunt | | 67.1 | 67.1 | 67.1 | 67.1 |
| $\tau_x$ ms | LR growth time | | 0.018 | 0.018 | 0.018 | 0.018 |
| $\tau_y$ ms | LR growth time | 0.1 | 0.01 | 0.01 | 0.01 | 0.01 |
| $\Delta\nu_y$, | incoher. tune spread | | 0.021 | 0.021 | 0.021 | 0.021 |
| $T$ | temperature, eV | | 92.2 | 69.1 | 92.2 | 69.1 |
| $N_{loss}/N_{tot}$ | lost per bunch | | 0.32 | 0.145 | 0.32 | 0.145 |
| Number of passes to saturat. | (high/low) SR | 8/25 | 7/18 | 15/39 | 7/18 | 15/39 |
| $P_{wall}$ W/m | power to the wall | 80. | 87. | 119. | 87. | 119. |
| $p_0$ | parameter | | 0.277 | 0.0694 | 0.277 | 0.0694 |
| $g$ | parameter | | 0.5529 | 0.743 | 0.553 | 0.7426 |
| norm | parameter $\int xdxe^{-V}$ | | 0.614 | 0.667 | 0.614 | 0.667 |
| $V_{max}$ | potent. bump, eV | | 0.8 | 0.8 | 0.8 | 0.8 |
| $\Delta$ | parameter | | 0.067 | 0.070 | 0.067 | 0.070 |

Table 3: Results of calculations for the four sets of parameters.